MATHEMATICAL MODELING AND COMPUTING, Vol. 11, No. 2, pp. 481–491 (2024)

A parallel preconditioning Schur complement approach for large scale industrial problems

Hassouna S.[1], Ramadane A.[2], Timesli A.[1], Azouani A.[3,4]

[1]*Hassan II University of Casablanca, National Higher School of Arts and Crafts (ENSAM Casablanca), AICSE Laboratory, 20670 Casablanca, Morocco*
[2]*Laboratory of Mathematics and Engineering Sciences, International University of Casablanca, Route Provinciale 3020, 50169, Casablanca, Morocco*
[3]*Sultan Moulay Slimane University, National School of Applied Sciences of Khouribga, LIPIM Laboratory, Khouribga, Morocco*
[4]*Institut für Mathematik I, Freie Universität Berlin, Arnimallee 7, 14195 Berlin, Germany*

(Received 7 January 2024; Revised 21 May 2024; Accepted 22 May 2024)

The purpose of this paper is to introduce a new strategy to improve the convergence and efficiency of the class of domain decomposition known as Schur complement techniques related to interface variables for the simulation of mechanical, electrical and thermal problems in presence of cross points. More precisely, we are interested not only in domain decomposition with two equal parts having the same physical properties but rather in more general splitting components. It is known that in the first case, the optimal convergence with good pre-conditioner is obtained in two iterations and the problem is still challenging in the second case. The primary goal then is to fill part of the gap in such problem domain decomposition techniques and to contribute to solve extremely difficult industrial problems of large scale by using parallel sparse direct solver of the multi-core environment of the whole system and handling each part of the system independently of the change of the mesh or the shifting of the mathematical method of resolution and subsequently, we treat the interface as boundary conditions. The numerical experiments of our algorithm are performed on few models arising from discretization of partial differential equations using Finite Element Method (FEM).

Keywords: *domain decomposition method; Schur complement; finite element method; parallel computing.*

2010 MSC: 15A09, 15A06, 15A23, 49M27, 11Y16 **DOI:** 10.23939/mmc2024.02.481

1. Introduction

Solving industrial problems using numerical methods usually leads to the assembly of large systems. This is all the more important in the context of multi-physics problems. For example, the study of an automotive engine implies the consideration of several state variables (hydraulic pressure, mechanical constraints, critical operating temperatures, electric current, etc.). Knowing that these variables interact with each other, the resulting systems are strongly coupled, of very large size and thus require a significant computation time. In the classical case, the replacement of a part in the example of the engine, leads us to recalculate all the subsystems because of the couplings. In the literature, we find several alternative techniques that consist in subdividing the domain into a succession of so-called artificial subdomains while defining the constitutive laws at the borders in order to ensure the continuity of the state variables [1]. Barboteu et al. [2,3] have used this method in the modeling of the hinges of rolling shutters. This problem is a real case of contact with friction, mono physical. The author subdivided the domain into several so-called artificial subdomains. Instead of obtaining a large global system, the problem has been transformed into several small systems that can be solved in a parallel way, while reducing the computation time. It is worth to note the importance of the contact interface definition and the laws of exchange in it. A contact interface can be considered as the union of boundaries con-

stituting the natural limit of different subdomains. At this interface, there is generally an exchange of certain physical quantities producing interactions of various kinds between boundaries. For example, the classical mechanical contact [4, 5], states that there is no interpenetration of the material at the interface and therefore, develops normal forces when the boundaries are brought into contact. The principle of action-reaction is interpreted here by the continuity of displacements and tensile stresses at the surface. There are also particular interface laws that are governed by phenomenological observations obtained from experimental tests. For example, the heat exchange law acting at the interface of two solids is a function of the contact conductance, which itself may be a function of the contact pressure [6, 7]. In this case, the equilibrium at the interface must respect the continuity of the flows but not that of the temperature. Finally, an electrical problem in the presence of interfaces implies the consideration of an electrical resistance governed by an interface law of the same nature as in thermal exchange, leading to continuity of current densities but not of voltage. Moreover, combining it with a pre-conditioner based on the FETI method [8], made this approach insensitive to discretization and the number of subdomains. An approach based on the FETI method [9] was proposed by Avery et al. His work allowed the solution of the frictionless contact problem with small displacements and contact areas known a priori. In the same framework, Dostal et al. [10] proposed algorithms for solving large deformation contact problems with friction in three dimensions. Some authors [2, 3, 11] have proposed a Newton–Schur algorithm which at each iteration of Newton allows solving by subdomains a linear problem condensed at the interfaces. The GMRES method [12] with generalized Neumann–Neumann preconditioner is applied to solve the local condensed subsystems at the interfaces of the subdomains. In such a context, the presence of many contact interfaces of various nature, the introduction of several unknowns related to the different physical fields, as well as the potential non-symmetry of the problem to be solved, clearly indicate the need to establish a generic approach for solving subdomains with so-called natural interfaces that would be applicable to a solution on computers with distributed memories.

To reduce the computation time, we propose an approach based on the notion of partial Schur complement. This approach has been used by Xing et al. and is inspired by works based on natural domain decomposition [13]. The authors treated the mechanical contact problem in a context of solving by an explicit dynamic method by partitioning the global matrix system into subsystems (subdomains) by highlighting the slave and master boundary nodes [13]. The linear system at each time step is solved in parallel by static condensation (Schur complement), reducing it to unknowns located at the domain boundaries. The approach proposed here allows addressing the generic solution of subdomain problems applicable to coupled contact problems. In this paper, we will only consider a thermal contact problem in two subdomains using finite element method.

2. Natural subdomain method

2.1. Classic definition of the interface

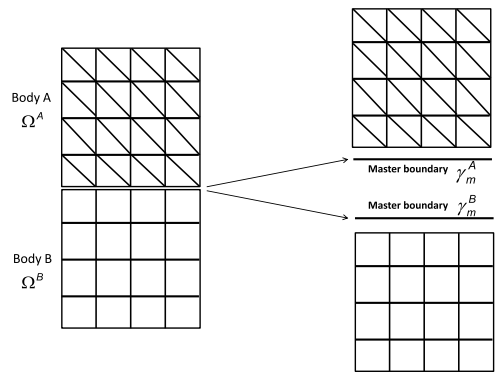

Fig. 1. Classic representation of contact boundaries.

In most of the literature [3, 13, 14], the contact problem is treated in a classical way (note here that the contact can be of any nature i.e. mechanical, thermal, thermoelectric, etc.). Consider the simple case illustrated in Figure 1. Let two solids A and B, of respective domains Ω^A and Ω^B and having different mesh densities. At the respective boundaries of these solids, noted γ^A and γ^B, are two subsets of elements noted respectively master and slave. The contact interface is then defined by the pair of boundaries noted $\gamma^A - \gamma^B$ whose respective mesh densities are dictated by those of the underlying solids.

Therefore, the boundaries γ^A and γ^B have different mesh densities. When considering the interaction between the subdomains, a coupling between the degrees of freedom associated with the boundaries γ^A and γ^B, naturally arises.

2.2. New definition of the interface

It is possible to define in a different way the link between the boundaries in contact. Figure 2 illustrates this approach. As defined earlier, each solid is meshed independently by adopting a master–slave approach. The mesh density of the slave boundary γ_s^α is dictated by the mesh density of the solid Ω^α where α denotes solid A or B. The mesh density of the master boundaries γ_m^α is independent of the solids. Then is defined, for each subdomain, the mesh of the solid as well as that of the contact interface $\gamma_s^\alpha - \gamma_m^\alpha$. When the interaction between two subdomains is taken into account when solving the global problem, it is important to define the boundaries through which, the subdomains will be coupled. From this point of view, the coupling that appears through the master boundaries γ_m^A and γ_m^B leads to a global matrix system in which there was, a priori, no interaction at these two boundaries. More details will be given later on.

This way of doing things has an important advantage compared to the classical approach presented in Figure 1. The subdomain Ω^A can be changed by another subdomain of different shape and having a different mesh density (see Figure 2), while keeping the contact interaction $\gamma_m^A - \gamma_m^B$. Only the local definition of the contact interface $\gamma_s^\alpha - \gamma_m^\alpha$ of the concerned subdomain is changed without affecting the links to the other subdomains. However, it is important to keep in mind that only one interface law can be assigned between the boundaries of contacting subdomains. This observation will bring an important nuance when defining the exchange laws at the interface compared to the classical approach.

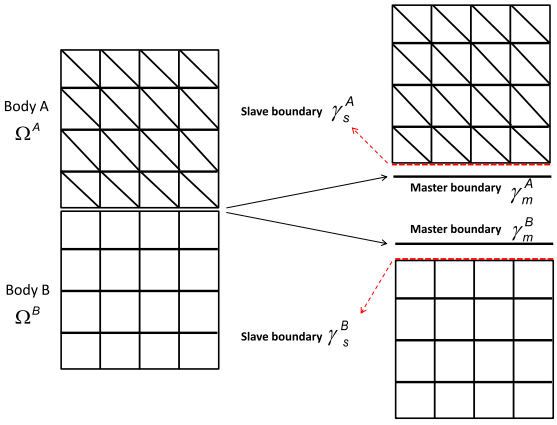

Fig. 2. New representation of contact boundaries.

Taking again the problem defined in Figure 2, it is easy to demonstrate that the system of equations, for a thermal, mechanical, etc. problem, can be written in the form:

$$\begin{pmatrix} \begin{pmatrix} K_{ii}^A & K_{is}^A & 0 \\ K_{ei}^A & K_{ss}^A & K_{sm}^A \\ 0 & K_{ms}^A & K_{mm}^A \end{pmatrix} & 0 \\ 0 & \begin{pmatrix} K_{ii}^B & K_{is}^B & 0 \\ K_{si}^B & K_{ss}^B & K_{sm}^B \\ 0 & K_{ms}^B & K_{mm}^B \end{pmatrix} \end{pmatrix} \begin{pmatrix} U_i^A \\ U_s^A \\ U_m^A \\ U_i^B \\ U_s^B \\ U_m^B \end{pmatrix} = \begin{pmatrix} F_i^A \\ F_s^A \\ F_m^A \\ F_i^B \\ F_s^B \\ F_m^B \end{pmatrix}, \tag{1}$$

where the index i represents the internal nodes of the solid excluding the nodes located on the slave boundary, and the indices s and m represent respectively the nodes belonging to the slave and master boundaries. The matrix K^α corresponds to the subdomain Ω^α, $\alpha = A, B$, and U^α is the vector of degrees of freedom of all elements of Ω^α. We distinguish the degrees of freedom of the master boundary U_m^α and slave boundary U_s^α from other internal degrees of freedom of the solid U_i^α. The system, as defined in (1) is not solvable because no link exists between the master boundaries with degrees of freedom U_m^A and U_m^B. It is therefore important to ensure continuity at the master interfaces. For example, the continuity of displacements if it is a mechanical contact, temperatures or voltages for the case of thermal and electrical contacts. In general, the continuity equation is written:

$$U_m^A - U_m^B = 0. \tag{2}$$

To satisfy the equilibrium conditions at the master interfaces (balance of forces in a mechanical problem or balance of thermal charges in a thermal transfer problem or of electrical charges in an electrical

problem), we use an iterative method that will correct the degrees of freedom of the master interfaces (displacements, temperature or voltage) allowing the respect of the equation:

$$F_m^A + F_m^B = 0. \tag{3}$$

In mechanics, the terms F_m^α are related to the nominal constraint which must satisfy the action-reaction principle but in an incremental sense, *i.e.* on the basis of a Newton iteration. In the case of thermal or electrical transfer, F_m^α is related respectively to the flux and current density, but in an incremental sense.

2.3. Resolution at the master–master interface

The thermal or electrical exchange at an interface consisting of two candidate contact boundaries on the continuous medium is then given by:

$$F_s^A = -F_s^B = h\left(U_s^A(x,y) - U_s^B(x,y)\right), \tag{4}$$

where h is the thermal or electrical contact conductance (considered constant in the linear problem), U^α is the temperature or voltage at the contacting solid boundary α, and (x,y) the coordinates related to the contacting surface. The flux leaving the surface γ^A is the opposite of that entering the surface γ^B. The variational form associated with equation (4), with the boundary γ^A being slave and γ^B master, is written:

$$W^C = \int_{\gamma^A} \left(\delta U^A - \delta U^B\right)\, h\left(U^A - U^B\right) d\gamma, \tag{5}$$

where δU^α is the weight associated with the boundary γ^α. In a finite element context, we will have:

$$\begin{aligned}
W^C &= \left\langle \delta U_n^A \right\rangle \left\{F^A\right\} + \left\langle \delta U_n^B \right\rangle \left\{F^B\right\},\\
\left\{F^A\right\} &= \left(\left[K_{AA}^C\right]\left\{U_n^A\right\} + \left[K_{AB}^C\right]\left\{U_n^B\right\}\right),\\
\left\{F^B\right\} &= \left(\left[K_{BA}^C\right]\left\{U_n^A\right\} + \left[K_{BB}^C\right]\left\{U_n^B\right\}\right),\\
\left[K_{\alpha\alpha}^C\right] &= h\int_{\gamma^A} \{N_\alpha\}\left\langle N_\alpha\right\rangle d\gamma, \quad \left[K_{\alpha\beta}^C\right] = -h\int_{\gamma^A} \{N_\alpha\}\left\langle N_\beta\right\rangle d\gamma.
\end{aligned} \tag{6}$$

Or N_α are the interpolation functions associated to the surface γ^α. F^α here represents the equivalent nodal flow on the boundary α. The upper subscript C indicates that this term comes from the contact. The previous equations are valid between two boundaries with a classical definition of master-slave contact. Introducing now the definition presented in Figure 2, a new definition of the incoming and outgoing flows between the master-slave pairs of each boundary associated with a solid becomes necessary. This new definition leads to the introduction of an a priori unknown thermal or electrical conductance. The latter is written:

$$F^A = \bar{h}\left(U_s^A - U_m^A\right), \quad F^B = \bar{h}\left(U_s^B - U_m^B\right). \tag{7}$$

At convergence, according to equation (2), we obtain:

$$U_m^A = U_m^B = \frac{1}{2}\left(U_s^A + U_s^B\right). \tag{8}$$

The equality of the real fluxes as defined in equation (4) and those defined in (7), allows to write with the help of (8):

$$F^A = \bar{h}\Big(U_s^A - \frac{1}{2}\left(U_s^A + U_s^B\right)\Big), \tag{9}$$

which allows us to deduce that $\bar{h} = 2h$. With this new definition, we can write, with the help of (6), the necessary relations for the new master-slave definition by subdomains:

$$W^{C,\alpha} = \int_{\gamma^\alpha} \left(\delta U_s^\alpha - \delta U_m^\alpha\right)\, \bar{h}\left(U_s^\alpha - U_m^\alpha\right) d\gamma, \tag{10}$$

$$\left\{F_s^\alpha\right\} = \left(\left[K_{ss}^{C,\alpha}\right]\left\{U_s^\alpha\right\} + \left[K_{sm}^{C,\alpha}\right]\left\{U_m^\alpha\right\}\right), \tag{11}$$

$$\left\{F_m^\alpha\right\} = \left(\left[K_{ms}^{C,\alpha}\right]\left\{U_s^\alpha\right\} + \left[K_{mm}^{C,\alpha}\right]\left\{U_m^\alpha\right\}\right), \tag{12}$$

where $\{U_s^\alpha\}$ and $\{U_m^\alpha\}$ are the respective degrees of freedom of the slave and master boundaries of the solid α and

$$\begin{aligned} \left[K_{\xi\xi}^{C,\alpha}\right] &= \bar{h}\left[M_{\xi\xi}^{\alpha}\right], & \left[K_{\xi\zeta}^{C,\alpha}\right] &= -\bar{h}\left[M_{\xi\zeta}^{\alpha}\right], \\ \left[M_{\xi\xi}^{\alpha}\right] &= \int_{\gamma^\alpha} \left\{N_\xi^\alpha\right\}\left\langle N_\xi^\alpha\right\rangle d\gamma, & \left[M_{\xi\zeta}^{\alpha}\right] &= \int_{\gamma^\alpha} \left\{N_\xi^\alpha\right\}\left\langle N_\zeta^\alpha\right\rangle d\gamma. \end{aligned} \tag{13}$$

With ξ and ζ being able to take the values of m and s. Therefore, $\{N_e^\alpha\}$ are the interpolation functions of the slave boundary of the solid γ^α. Note here that the restriction of the identical mesh of two master boundaries implies, a fortiori that $\left\{N_m^A\right\} \equiv \left\{N_m^B\right\}$. The application of relation (3) finally allows us to write the equilibrium at the master boundaries according to which:

$$\{R\} = \left\{F_m^A\right\} + \left\{F_m^B\right\} = \{0\}. \tag{14}$$

In a subdomain resolution context, relation (14) will be satisfied by an iterative method. For this purpose, it is assumed that the resolution on each subdomain has been obtained by admitting a fixed value of $\{U_m^\alpha\}$ thus allowing the displacement of the slave boundary to be estimated using the system (1) for a resolution on each subdomain:

$$\begin{bmatrix} K_{ii}^\alpha & K_{is}^\alpha \\ K_{si}^\alpha & K_{ss}^\alpha \end{bmatrix} \begin{Bmatrix} U_i^\alpha \\ U_s^\alpha \end{Bmatrix} + \begin{bmatrix} 0 \\ K_{sm}^\alpha \end{bmatrix} \{U_m^\alpha\} = \begin{Bmatrix} F_i^\alpha \\ F_s^\alpha \end{Bmatrix}, \tag{15}$$

where the terms ii are related to the solid variational form term α, $\{F_i^\alpha\}$ contains the Neumann boundary conditions and the volume stresses applied on the solid and

$$[K_{ss}^\alpha] = \left[K_{ss}^{B,\alpha}\right] + \left[K_{ss}^{C,\alpha}\right], \quad [K_{is}^\alpha] = \left[K_{is}^{B,\alpha}\right]. \tag{16}$$

Knowing the value of $\{U_s^\alpha\}$ for each subdomain, it is possible to compute the residual defined in (14) to obtain a correction to the solution to the field $\{U_m^\alpha\}$ by:

$$[K_{ss}^\alpha] = \left[K_{ss}^{B,\alpha}\right] + \left[K_{ss}^{C,\alpha}\right], \quad [K_{is}^\alpha] = \left[K_{is}^{B,\alpha}\right], \tag{17}$$

$$\{R_m\} = \frac{1}{2}\sum_{\alpha=1}^{2} \{F_m^\alpha\}, \tag{18}$$

$$\left\{U_m^{\alpha,i}\right\} \equiv \left\{U_m^i\right\} = \left\{U_m^{i-1}\right\} + \left\{\Delta U_m^i\right\}, \tag{19}$$

$$\left\{\Delta U_m^{A,i}\right\} = \beta\left\{\overline{\Delta U}_m^{A,i}\right\} + (1-\beta)\left\{\overline{\Delta U}_m^{B,i}\right\}, \tag{20}$$

$$\left\{\Delta U_m^{B,i}\right\} = \beta\left\{\overline{\Delta U}_m^{B,i}\right\} + (1-\beta)\left\{\overline{\Delta U}_m^{A,i}\right\}, \tag{21}$$

$$\left\{\overline{\Delta U}_m^{\alpha,i}\right\} = -\left[K_C^\alpha\right]^{-1}\{R_m\}, \quad \alpha = A, B, \tag{22}$$

where $[K_C^\alpha]^{-1}$ is a correction matrix to be defined. The idea behind this method is to find the correction of the displacement of each boundary from the common residue $\{R_m\}$ and to apply relation (2) through a mixing law defined by relations (20) and (21). In the case where $\beta = 1/2$, we simply average the corrections obtained from two "master" boundaries. The value of β can be defined as a function of physical quantities (see the numerical applications section). Note, for now, that if two subdomains have the same dimensions, the same mesh density and the same physical parameters (same thermal or electrical conductivity), then the optimal value for this parameter is 1/2.

3. Definition of the correction matrix at the interface based on the subdomain flexibility

The correction matrix at the interface can be defined in various ways. The following lines present two distinct techniques, either the direct method or the method based on the subdomain flexibility. It is possible to define the correction matrix $[K_C^\alpha]^{-1}$ exactly by using the system of equations (1) adapted to the master-slave approach presented in the previous section and such that:

$$[K_{mm}^\alpha]\{U_m^\alpha\} + [K_{ms}^\alpha]\{U_s^\alpha\} = [F_m^\alpha], \tag{23}$$

$$[K_C^\alpha]^{-1} \equiv [K_{mm}^\alpha]^{-1} = \frac{1}{\bar{h}}[M_{mm}]^{-1}, \tag{24}$$

or the matrix $[M_{mm}]$ is as defined in equation (13). One can notice, in the denominator of equation (24), a term in $\bar{h} = 2h$. If the value of the physical parameter h becomes large, this approximation of the

interface correction matrix will make the iterative process very slow. Here we propose an alternative to the definition of $[K_C^\alpha]$ based on the following idea. By applying the residual $\{R_m\}$ not on the master-master interface but on the solid, we can obtain a good estimate of the correction of the nodal variables carried by the master boundaries. Since a coincident node-to-node mesh necessarily implies the same mesh density of the master and slave boundaries, the residual $\{R_m\}$ at the nodes of the master-master interface can be applied to the nodes of the slave interface of the solid. Therefore, it is possible to take as a first approximation of $[K_C^\alpha]$:

$$\left[K_C^\alpha\right] = \left[\bar{K_{ss}^\alpha}\right] = \left[K_{ss}^{B,\alpha}\right] - \left(\left[K_{si}^{B,\alpha}\right]\left[K_{ii}^\alpha\right]^{-1}\left[K_{is}^{B,\alpha}\right]\right). \tag{25}$$

For which the contributions of the contact interface to the global matrix of the subdomain in question are not assembled. The matrix $\left[\bar{K_{ss}^\alpha}\right]$ is therefore the result of a static condensation of the global matrix of the subdomain commonly referred to as the Schur complement. Since the computation of the matrix $\left[\bar{K_{ss}^\alpha}\right]$ is costly, it is possible to limit the dimension of $\left[\bar{K_{ii}^\alpha}\right]$ by taking only a certain number of rows of elements under the slave boundary surface. However, the mesh density to be discarded inevitably has the convergence of this method as will be illustrated in the next section.

4. Numerical applications

This section summarizes the numerical results of the Parallel Preconditioning Schur Complement (PPSC) for the solid-solid thermal contact problem between two bars, denoted A and B (see Figure 3). Each bar $\alpha = A, B$ has conductivity K_α, cross-section $S_\alpha = \pi r_\alpha^2$ and length L_α.

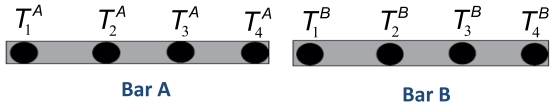

Fig. 3. One-dimensional thermal contact problem.

We consider a thermal contact conductance $h = \frac{K_{moy}\times S_{moy}}{L_{moy}} \times C$ between the two bars with $K_{moy} = \frac{K_A+K_B}{2}$, $S_{moy} = \frac{S_A+S_B}{2}$, $L_{moy} = \frac{L_A+L_B}{2}$ and C is the order of magnitude of thermal conductivity. As shown in Figure 4, two subsystems can be written in the form:

$$\begin{pmatrix} 4\frac{K_\alpha}{L_\alpha} & -4\frac{K_\alpha}{L_\alpha} & 0 & 0 & 0 \\ -4\frac{K_\alpha}{L_\alpha} & 8\frac{K_\alpha}{L_\alpha} & -4\frac{K_\alpha}{L_\alpha} & 0 & 0 \\ 0 & -4\frac{K_\alpha}{L_\alpha} & 8\frac{K_\alpha}{L_\alpha} & -4\frac{K_\alpha}{L_\alpha} & 0 \\ 0 & 0 & -4\frac{K_\alpha}{L_\alpha} & 4\frac{K_\alpha}{L_\alpha}+h & -h \\ 0 & 0 & 0 & -h & h \end{pmatrix} \begin{pmatrix} T_1^\alpha \\ T_2^\alpha \\ T_3^\alpha \\ T_s^\alpha \\ T_m^\alpha \end{pmatrix} = \begin{pmatrix} F_1^\alpha \\ F_2^\alpha \\ F_3^\alpha \\ F_s^\alpha \\ F_m^\alpha \end{pmatrix}, \quad \alpha = A, B. \tag{26}$$

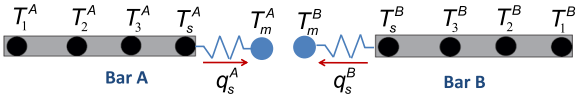

Fig. 4. Discrete representation at the contact interface.

We notice that the term at position $(4, 4)$ of the matrix $\left[K^\alpha\right]$ contains both the contribution coming from element 3 (see Figure 4) and that coming from the master-slave interface of this subdomain,

$$\begin{pmatrix} K_{ii}^\alpha & K_{is}^\alpha & 0 \\ K_{is}^\alpha & K_{ss}^\alpha & K_{sm}^\alpha \\ 0 & K_{sm}^\alpha & K_{mm}^\alpha \end{pmatrix} \begin{pmatrix} T_i^\alpha \\ T_s^\alpha \\ T_m^\alpha \end{pmatrix} = \begin{pmatrix} F_i^\alpha \\ F_s^\alpha \\ F_m^\alpha \end{pmatrix}, \quad \alpha = A, B, \tag{27}$$

where

$$\left[K_{ii}^\alpha\right] = \begin{pmatrix} 4\frac{K_\alpha}{L_\alpha} & -4\frac{K_\alpha}{L_\alpha} & 0 \\ -4\frac{K_\alpha}{L_\alpha} & 8\frac{K_\alpha}{L_\alpha} & -4\frac{K_\alpha}{L_\alpha} \\ 0 & -4\frac{K_\alpha}{L_\alpha} & 8\frac{K_\alpha}{L_\alpha} \end{pmatrix}, \; K_{is}^\alpha = -4\frac{K_\alpha}{L_\alpha}, \; K_{ss}^\alpha = 4\frac{K_\alpha}{L_\alpha} + h, \; K_{sm}^\alpha = -h, \; K_{mm}^\alpha = h. \tag{28}$$

Two subsystems can be rewritten as:

$$\begin{pmatrix} K_{ii}^\alpha & K_{is}^\alpha \\ K_{si}^\alpha & K_{ss}^\alpha \end{pmatrix} \begin{pmatrix} T_i^\alpha \\ T_s^\alpha \end{pmatrix} + \begin{pmatrix} 0 \\ K_{sm}^\alpha \end{pmatrix} T_m^\alpha = \begin{pmatrix} F_i^\alpha \\ F_s^\alpha \end{pmatrix}, \quad \alpha = A, B, \tag{29}$$

or in the following condensed form:

$$\left[K^\alpha\right]\{T^\alpha\} + \{K_{sm}^\alpha\} T_m^\alpha = \{F^\alpha\}, \quad \alpha = A, B. \tag{30}$$

We can establish the residue expression $\{R_m\}$ at the interface of the subdomains using equation (18) such that:

$$F_m^\alpha = -\bar{h}\,(T_e^\alpha - T_m^\alpha)\,. \tag{31}$$

Now, the parameter β is equal to 0.5 if the subdomains were of the same dimension, mesh density and defined with the same physical parameters. Recall that this parameter weights the update of the correction of the nodal variables associated with the master boundaries in order to hopefully converge faster to the solution $\{T_m^{A,i}\} = \{T_m^{B,i}\}$. However, if any of the subdomains involved are different in nature, it is clear that the optimal value of β will no longer be 0.5. The objective of this section is to propose a good estimate of this parameter. Intuitively, we can deduce that the parameter must be established according to the relative stiffness of the bodies potentially in contact. This observation allows us to establish the first expression linking the material property of the subdomains and a certain amount of material such that:

$$\beta = \frac{\frac{K_A}{h_A}}{\frac{K_A}{h_A} + \frac{K_B}{h_B}}, \tag{32}$$

where K_A and K_B are respectively the thermal conductivities of the subdomains A and B, and h_A and h_B are the characteristic sizes of an element of the subdomains A and B.

Another approach to take into account this internal stiffness is to take the trace of the matrices of subdomains A and B excluding the contact contributions such that:

$$\beta = \frac{\frac{\mathrm{tr}([K^A])}{n_A}}{\frac{\mathrm{tr}([K^A])}{n_A} + \frac{\mathrm{tr}([K^B])}{n_B}}, \tag{33}$$

where n_A and n_B are the numbers of points (called nodes in FEM) of discretization in the subdomains A and B.

We recall that the trace operator allows us to take into account the effect of the dominant terms in the tangent matrix and, by the same token, of the nature of the materials, of the quantity of material considered as well as of all the non-linear exchange phenomena at the boundaries.

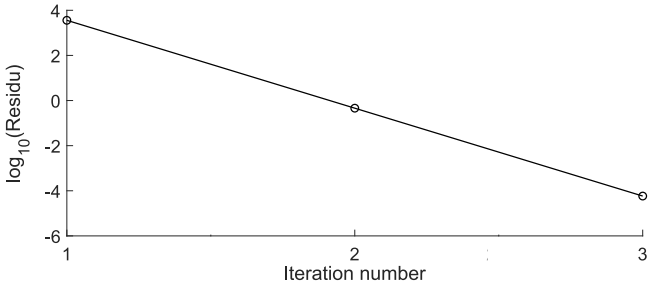

Fig. 5. Evolution of residual as a function of iterations in the case of 5 nodes per subdomain.

For numerical applications, consider two steel bars A and B of thermal conductivity $K_A = K_B = 36\,\mathrm{W/(m{\cdot}K)}$. The lengths of the bars are $L_A = L_B = 1\,\mathrm{m}$ and the radii of its circular sections are $r_A = r_B = 5\,\mathrm{cm}$. The temperatures of the edges of two bars are $T_1^A = T(x=0) = 100°\mathrm{C}$ and $T_1^B = T(x = 1\,\mathrm{m}) = 0°\mathrm{C}$. We consider a contact conductance $h = 10^6 \times \frac{K_A \times S_A}{L_A}$. Note that when the thermal contact conductance h tends to infinity, two bars can be considered as a homogeneous bar, so we can compare the results of the PPSC method with those of the analytical solution $T_{exact}(x) = \frac{T(L)-T(0)}{L}x + T(0)$. For more precision, we calculate the relative error $\left(\frac{\|T_{PPSC} - T_{exact}\|}{\|T_{exact}\|} \times 100\ (\%)\right)$ at the contact position.

Figure 6 shows the outstanding performance of using Schur's complement in preconditioning. The algorithm converged after 3 loops by reaching a residual on the order of 10^{-6}. The number of iterations can vary depending on the mesh parameters and geometry.

The analysis of Table 1 shows that the number of iteration re-

Table 1. Influence of discretization in two subdomains considering $h = 10^6 \times \frac{K_A \times S_A}{L_{moy}}$ ($S_{moy} = S_A$ and $K_{moy} = K_A$).

L_A	L_B	n_A	n_B	Number of iterations	Relative error (%)
0.5	0.5	3	3	3	1.6207×10^{-6}
0.5	0.5	5	5	3	1.6207×10^{-6}
0.5	0.5	7	7	3	1.6207×10^{-6}
0.5	0.5	11	11	3	1.6207×10^{-6}
0.5	0.5	15	15	3	1.6207×10^{-6}
0.5	0.5	3	5	3	1.6207×10^{-6}
0.25	0.75	3	3	4	4.2×10^{-3}
0.25	0.75	3	5	21	4.2×10^{-3}

mains insensitive when the two bars have the same length while it increases significantly when the two lengths are different.

Figure 6 shows good results for the subdomain method when comparing with the analytical solution. Indeed, the case (a) corresponds to the homogeneous case where two bars have the same mesh and the same geometry. The resulting master temperature is naturally 50.5°C, the same as indicated by the analytical solution. The linearity of the solution and the respect of the boundary conditions confirm the validity of the solution as well as the efficiency of the Schur complement conditioning and its coupling to the FEM. Case (c) is an application of a special case where the length of the bar B is 4 times that of A as well as a different mesh. Despite the large number of iterations required in this case, the result is identical to the analytical one and gives the high interface temperature (75°C), given the short length of the hot bar (A).

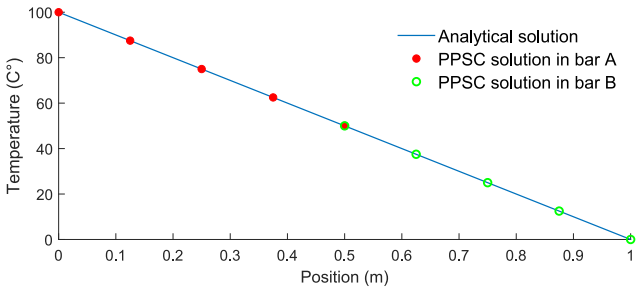

a ($L_A = 0.5\,\text{m}$, $L_B = 0.5\,\text{m}$, $n_A = 5$ and $n_B = 5$)

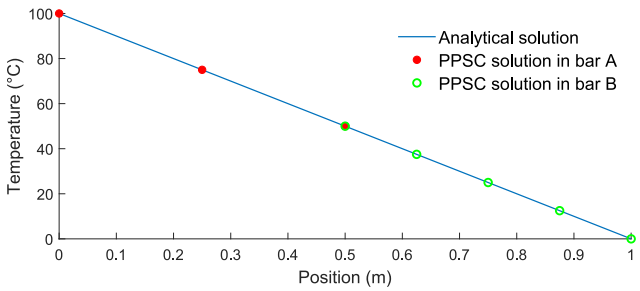

b ($L_A = 0.5\,\text{m}$, $L_B = 0.5\,\text{m}$, $n_A = 3$ and $n_B = 5$)

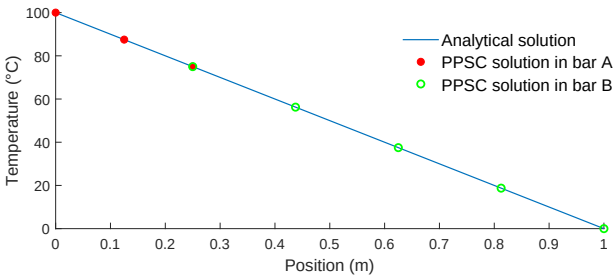

c ($L_A = 0.25\,\text{m}$, $L_B = 0.75\,\text{m}$, $n_A = 3$ and $n_B = 5$)

Fig. 6. Comparison of the results of the PPSC method and those analytical ones.

Now we plot the effect of the contact thermal conductance in Figure 7. We observe that the decrease in the order of magnitude of the conductance at the interfaces increases the difference of two temperatures at the interfaces. The conductance at the interface intervenes in the equation of the exchange law between two bodies and can be assimilated to a transmission coefficient of the physical quantity which is, in our case, the temperature. The more this constant is important, the more there is exchange of heat flow and this ensures a good diffusion and continuity of temperature. Thus, in the case where h is of the order of 100, the discontinuity reached 60°C of deviation and from $ho10^6$, we observe that the temperature is continuous and the bar can be assimilated to the homogeneous case and the values are the same as in the analytical case.

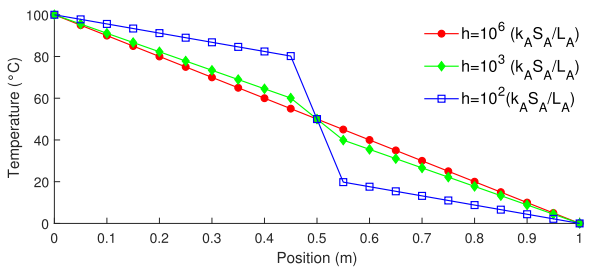

Fig. 7. Effect of contact conductance.

In order to understand the effect of the conductivity coefficient, we considered the same mesh and geometry (the a case) for both steel and aluminum bars. Figure 8 shows a dominance of the bar with the higher conductivity coefficient, i.e. bar B. Thus, the equilibrium temperature at the interface is close to 20°C and remains dominated by the cold bar. The same is true for the effect of the length of the bars, those with the largest dimensions have a greater dominance on the contact temperature.

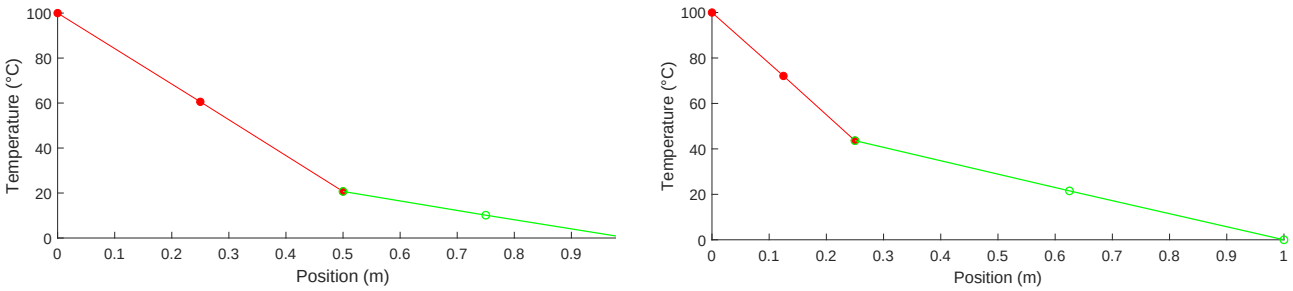

a ($L_A = 0.5\,\mathrm{m}$ and $L_B = 0.5\,\mathrm{m}$) ***b*** ($L_A = 0.25\,\mathrm{m}$ and $L_B = 0.75\,\mathrm{m}$)

Fig. 8. Results in the case $n_A = 3$, $n_B = 5$ and $h = 10^4 \times \frac{K_{moy} \times S_{moy}}{L_{moy}}$.

Table 2 summarizes the simulation results of an aluminum and steel bar by coupling the Schur complement preconditioning and the finite element method. The results show good convergence after a few iterations not exceeding 10 iterations and reaches a residual on the order of 10^{-6}. The number of iterations remains highly dependent on the mesh. This method is dedicated to meshes of large size, that is why we present in Table 2 the results of the simulations with a large number of meshes, which show some iterations not exceeding 10 iterations.

Table 2. Results from two different materials for $h = 10^4 \times \frac{K_{moy} \times S_{moy}}{L_{moy}}$.

L_A	L_B	n_A	n_B	Number of iterations	Residu
0.5	0.5	3	3	6	4.8686×10^{-6}
0.5	0.5	3	5	15	2.7134×10^{-5}
0.5	0.5	3000	5000	10	9.2288×10^{-5}
0.5	0.5	5000	5000	6	4.8686×10^{-6}
0.25	0.75	3	3	6	1.7816×10^{-6}
0.25	0.75	3	5	9	1.0997×10^{-5}
0.25	0.75	3000	5000	7	4.4473×10^{-5}
0.25	0.75	5000	5000	6	1.7815×10^{-6}

5. Conclusion

In this paper, a novel method for solving contact problems by natural subdomains is presented. In order to achieve subdomain independence, the interface discretization is based on a modified master-slave approach. In this approach, the set of contact candidate boundaries are identified as slaves and the interface generated via two virtual master boundaries, each of which is coupled with its slave boundary. In this context, the global resolution of the linear system, or linearized at each Newton iteration, is obtained after convergence of all interfaces. To do this, two methods were proposed for the calculation of the correction matrix at the interface. The first method, called direct, depends exclusively on the physical properties of the interface. Depending on the law governing the interface, the convergence can become very slow. The second method is based on the flexibility of the candidate subdomains at the contact. Thus, it allows to consider the nature of the bodies in contact. However, taking into account the whole body requires a significant computation time. The use of the trace operator was particularly interesting to converge with a minimum computational cost for any choice of mesh. Numerical examples in 1D have demonstrated the efficiency of this method, which is very promising for the resolution of large-scale problems with industrial impact. Work is currently in progress to apply the proposed method to the resolution of multiphysics problems by subdomains.

[1] Quarteroni A., Valli A. Domain Decomposition Methods for Partial Differential Equation. Clarendon Press, Oxford (1999).

[2] Barboteu M. Contact, frottement et techniques de calcul parallèle. Thèse de doctorat, Université Montpellier II (1999).

[3] Barboteu M., Alart P., Vidrascu M. A domain decomposition strategy for non classical frictional multicontact problems. Computer Methods in Applied Mechanics and Engineering. **190** (37–38), 4785–4803 (2001).

[4] Marceau D. Modélisation du contact tridimensionnel avec frottement en grandes transformations et son application à l'étude des dispositifs d'ancrage multitorons. Thèse de doctorat, Département de génie civil, Université Laval (2001).

[5] Marceau D., Fafard M., Bastien J. Constitutive law for wedge-tendon gripping interface in anchorage device-numerical modeling and parameters identification. Structural Engineering and Mechanics. **15** (6), 609–628 (2003).

[6] Goulet P. Modélisation du comportement thermo-électro-mécanique des interfacesde contact d'une cuve de Hall-Héroult. Thèse de doctorat, Département de génie chimique, Université Laval (2003).

[7] Richard D. Aspects thermomécaniques de la modélisation par éléments finis dupréchauffage électrique d'une cuve de Hall-Héroult: Lois constitutives, conception orientée objet et validation. Thèse de doctorat, Département de génie civil, Université Laval (2004).

[8] Farhat C., Roux F.-X. A method of finite element tearing and interconnecting its parallel solution algorithm. International Journal for Numerical Methods in Engineering. **32** (6), 1205–1227 (1991).

[9] Avery P., Rebel G., Lesoinne M., Farhat C. A numerically scalabel dual-primalsubstructuring method for the solution of contact problems – part I: the frictionless case. Computer Methods in Applied Mechanics and Engineering. **193** (23–26), 2403–2426 (2004).

[10] Dostál Z., Horák D., Kučera R., Vondrák V., Haslinger J., Dobiáš J., Pták S. FETI based algorithms for contact problems: scalability, large displacements and 3D Coulomb friction. Computer Methods in Applied Mechanics and Engineering. **194** (2–5), 395–409 (2005).

[11] Kalantzis V. A spectral Newton–Schur algorithm for the solution of symmetric generalized eigenvalue problems. Electronic Transactions on Numerical Analysis. **52**, 132–153 (2020).

[12] Saad Y. Method for Sparse Linear Systems. Second ed. with corrections (2000).

[13] Xing H. L., Fujumoto T., Makinouchi A. Static-explicit fe modeling of 3-D large deformation multibody contact problems on parallel computer. Simulation of Materials Processing: theory Methods and Applications. 207–212 (1998).

[14] Mandel M. Balancing domain decomposition. Communications in Applied Numerical Methods. **9** (3), 233–241 (1993).

Паралельний підхід попереднього зумовлення Шура для великомасштабних промислових задач

Хассуна С.[1], Рамадан А.[2], Таймеслі А.[1], Азуані А.[3,4]

[1] *Університет Хасана II Касабланки, Національна вища школа мистецтв і ремесел (ENSAM Касабланка), AICSE лабораторія, 20670 Касабланка, Марокко*
[2] *Лабораторія математики та інженерних наук Міжнародного університету Касабланки, Провінційна дорога 3020, 50169, Касабланка, Марокко*
[3] *Університет Султана Мулая Слімана, Національна школа прикладних наук Хурібга, LIPIM лабораторія, Хурібга, Марокко*
[4] *Інститут математики I, Вільний університет Берліна, Arnimallee 7, 14195 Берлін, Німеччина*

Метою цієї роботи є впровадження нової стратегії для покращення збіжності та ефективності класу декомпозиції доменів, відомого як методи доповнення Шура, які пов'язані з інтерфейсними змінними для моделювання механічних, електричних і теплових задач за наявності точок перетину. Точніше, нас цікавить не лише розкладання домену на дві однакові частини з однаковими фізичними властивостями, але і більш загальні компоненти розщеплення. Відомо, що в першому випадку оптимальна збіжність з хорошим попереднім зумовленням досягається за дві ітерації, а в другому випадку задача залишається складною. Тоді основна мета полягає в тому, щоб заповнити частину прогалини серед таких методів декомпозиції області задачі та сприяти вирішенню надзвичайно складних промислових задач великого масштабу за допомогою паралельного розрідженого прямого розв'язувача багатоядерного середовища всієї системи та обробки кожної частини системи незалежно від зміни сітки або зсуву математичного методу розв'язування, і після того розглядаючи межу поділу як граничні умови. Чисельні експерименти нашого алгоритму виконуються на декількох моделях, що виникають із дискретизації диференціальних рівнянь у частинних похідних за допомогою методу скінченних елементів (FEM).

Ключові слова: *метод декомпозиції області; доповнення Шура; метод скінченних елементів; паралельні обчислення.*